our experiments it is evident that the formation of vacancy-impurity complexes in Si depends on the charge states of the defects. (5) Our results are consistent with the argument that the 175°K stage is due to the migration of the neutral vacancy and the 350°K stage is due to the annealing of some secondary defects, among which there are various vacancy-impurity complexes.

ACKNOWLEDGMENT

The authors wish to express their appreciation to M. L. Swanson for his valuable comments on this work.

PHYSICAL REVIEW B VOLUME 1, NUMBER 4 15 FEBRUARY 1970

Far-Infrared Properties of Lattice Resonant Modes. III. Temperature Effects*

R. W. ALEXANDER, JR.,† A. E. HUGHES,‡§ AND A. J. SIEVERS
Laboratory of Atomic and Solid State Physics, Cornell University, Ithaca, New York 14850
(Received 10 October 1969)

We have measured the temperature-dependent absorption spectrum associated with resonant modes in KBr:Li^+, NaCl:Cu^+, KI:Ag^+, and MnF_2:Eu^{2+}. A comparison is given of the measured temperature dependence with that expected from a linear-coupling theory using the known static stress coupling coefficients. We find that the linear-coupling model is capable of explaining the measured temperature dependences provided the active resonant mode is coupled to another inactive resonant mode, but not if the coupling is to a Debye spectrum of lattice modes.

I. INTRODUCTION

TEMPERATURE-DEPENDENCE studies of the far-infrared absorption spectra from low-lying resonant modes can be used to measure the anharmonic nature of weakly bound impurities in crystals. In the harmonic approximation, the normal modes of a lattice containing a heavy mass defect can be considered to consist of a resonant mode Q and a set of other lattice modes q. Strictly speaking, the resonance is not a single mode, but when it occurs at low frequency as a sharp peak in the density of states, it is a reasonable approach to regard the resonance as being in a single mode. If only the mode Q is infrared-active, the absorption spectrum consists of a single sharp line at frequency Ω which is temperature independent.

Previously, we have used this approach to characterize the isotope shift[1] and stress shift[2] experiments on infrared active resonant modes associated with impurities which are weakly coupled to the host lattice (hereafter referred to as I and II, respectively). In this paper we describe temperature-dependent properties observed in practice and attempt to explain their presence in terms of various anharmonic effects.

The first investigations of the temperature-dependent properties of resonant modes presented some puzzling results. With increasing temperature, the center frequency of the impurity-induced absorption line decreased, the linewidth increased and the integrated absorption intensity decreased for both KI:Ag^+ and KBr:Li^+.[3] On the other hand, for NaCl:Cu^+ although similar temperature dependences were observed for the center frequency and the linewidth, the integrated absorption intensity was almost independent of temperature.[4] Attention then focused on the most dramatic effect, the temperature dependence of the integrated absorption and a great deal of confusion followed because it was not clear how much of the absorption spectrum was being considered in each experiment.

In discussing the intensity of the integrated absorption due to the resonant mode it is important to be quite clear as to how much of the absorption spectrum is being discussed. As stated previously if the potential energy is purely harmonic the spectrum consists of a sharp single line at Ω. When anharmonic terms are included this line may shift, broaden, and change in strength, but in general the anharmonicity would also induce other lines to appear elsewhere in the spectrum. These may be described in the language of molecular spectroscopy as combination bands, overtones, etc., or in solid-state terms as sidebands, two-phonon transi-

* This work has been supported by the U. S. Atomic Energy Commission under Contract No. AT(30-1)-2391, Technical Report No. NYO-2391-101. Additional support was received from the Advanced Research Projects Agency through the Materials Science Center at Cornell University, Report No. 1256.
† Present address: Physikalisches Institut der Universität Freiburg, 7800 Freiburg Im Breisgau, West Germany.
‡ Harkness Fellow of the Commonwealth Fund of New York, on leave from the Atomic Energy Research Establishment, Harwell, Didcot, Berkshire, United Kingdom.
§ Present address: Atomic Energy Research Establishment, Harwell, Didcot, Berkshire, United Kingdom.
[1] R. D. Kirby, I. G. Nolt, R. W. Alexander, Jr., and A. J. Sievers, Phys. Rev. **168**, 1057 (1968).
[2] I. G. Nolt and A. J. Sievers, Phys. Rev. **174**, 1004 (1968).
[3] S. Takeno and A. J. Sievers, Phys. Rev. Letters **15**, 1020 (1965).
[4] R. Weber and P. Nette, Phys. Letters **20**, 493 (1966); R. Weber and F. Siebert, Z. Physik **213**, 273 (1968).

tions, etc. The original line near Ω would then be referred to as the "fundamental," or as we prefer, the zero-lattice-phonon (ZLP) line. We are concerned with the intensity of this line only, and not with the complete absorption spectrum associated with the resonant mode. In fact it can be shown[5] that if the complete spectrum is taken into account then

$$\int \alpha(\omega)d\omega = \text{const}. \tag{1}$$

This "sum rule" is exact for an anharmonic system with a linear dipole moment, and a simple proof appears in *Appendix A*. In contrast, we are interested in the temperature dependence of the quantity $I(T)$, where

$$I(T) = \int_{\text{ZPL}} \alpha(\omega)d\omega. \tag{2}$$

Historically, the first attempted explanation of the temperature dependence of the ZPL intensity[3] made use of the well developed theory for the intensity of electronic transitions at impurities in crystals, when coupling to the lattice modes is considered. This problem is itself frequently referred to as the optical analogue of the Mossbauer effect,[6] and has received extensive coverage in the literature.[7–10]

The essential results of the electronic theory are the following. If the electronic transition energy is assumed to depend linearly and quadratically on the phonon coordinates, then it is found that the spectrum consists of a sharp line (zero-phonon line) plus broader phonon-assisted sidebands. The temperature dependence of the zero-phonon line is qualitatively similar to that observed for the resonant modes. Quantitatively, the main result of the theory is that the intensity of the zero-phonon line when only linear coupling is included in given by[7]

$$I(T) = e^{-\gamma}, \tag{3}$$

with

$$\gamma = \sum_{q} S_q(2\bar{n}_q + 1), \tag{4}$$

where S_q is a dimensionless linear coupling parameter usually known as the Huang–Rhys factor. The exponential form of $I(T)$ has lead to the use of the term "Debye–Waller factor" in describing the temperature dependence. The temperature dependence of an electronic transition, the R_2 band in KCl has been treated successfully in this manner.[11,12] A similar calculation has also been made for a localized mode, the U center in KCl, using the data of Fritz *et al.*[13,14] In this case there is good reason to believe that the electronic theory is applicable.[15,16] It is not yet clear whether this theory can justifiably be applied to the case of the resonant mode. One of the purposes of this paper is to compare the measured temperature dependence with that expected from a linear-coupling theory using the known static-stress coupling coefficients to calculate the coupling of the system to the dynamical strains, i.e., the lattice modes.

In Sec. II we report temperature-dependent measurements of resonant modes at higher resolution than used in previous studies. Most of the studies were made on KBr:LiBr, NaCl:CuCl, and KI:AgI with the crystals containing isotopically pure dopants. Some measurements for a resonant mode in MnF_2:Eu^{2+} are also presented here.

In Sec. III we compare the measured temperature dependence of the linewidth and the center frequency with that derived from anharmonic effects. Good agreement is found as long as low-frequency phonons play the dominant role. We then show that linear coupling of a Debye spectrum of phonons with the known coupling coefficients does not explain the observed change in the integrated intensity. Somewhat better agreement is obtained, however, if linear coupling to an even resonant mode is assumed.

Finally, in Sec. IV we speculate on the applicability of a linear-coupling model for lattice-resonant modes.

II. EXPERIMENT

A. Procedures

Our first measurements of the temperature effects of doped alkali halides were made with a grating monochromator which required three grating and filter changes to measure the frequency region from 10 to 50 cm^{-1}.[3] These grating changes together with the problem of second-order radiation have introduced experimental uncertainty in the identification of broad resonances which may appear as the integrated intensity of the ZPL decreases with increasing temperature. To overcome this problem we have used the Strong-type lamellar interferometer described in II to investigate temperature effects. In one pass, the frequency interval from 10 to 50 cm^{-1} can be measured. Also because of the large throughput of this instru-

[5] D. Strauch, Phys. Status Solidi **33**, 397 (1969).
[6] R. H. Silsbee and D. B. Fitchen, Rev. Mod. Phys. **36**, 432 (1964).
[7] A. A. Maradudin, in *Solid State Physics*, edited by F. Seitz and D. Turnbull (Academic Press Inc., New York, 1967), Vol. 18.
[8] M. Lax, J. Chem. Phys. **5**, 221 (1964).
[9] D. E. McCumber, Phys. Rev. **135**, A1676 (1964).
[10] R. H. Silsbee, in *Optical Properties of Solids*, edited by S. Nudelman and S. S. Mitra (Planeum Press, Inc., New York, 1969).
[11] D. B. Fitchen, R. H. Silsbee, T. A. Fulton, and E. L. Wolf, Phys. Rev. Letters **11**, 275 (1963).
[12] R. H. Silsbee, Phys. Rev. **138**, A180 (1965).
[13] B. Fritz, U. Gross, and D. Bauerle, Phys. Status Solidi **11**, 231 (1965).
[14] B. Fritz, in *Localized Excitations in Solids*, edited by R. F. Wallis (Plenum Press, Inc., New York, 1968).
[15] A. E. Hughes, Phys. Rev. **173**, 860 (1968).
[16] I. P. Ipatova, A. V. Shubashiev, and A. A. Maradudin, in *Localized Excitations in Solids*, edited by R. F. Wallis (Plenum Press, Inc., New York, 1968).

ment,[17] measurements at a factor 5 higher resolution have been possible. For low-temperature samples, the transmission spectrum was determined with a resolution of 0.18 cm^{-1}. At sample temperatures above 30°K, where the absorption lines are quite broad, a resolution of 0.36 cm^{-1} was used.

The impurity-induced absorption coefficient was obtained in the usual manner by dividing the transmission spectrum of the doped sample by the transmission of the pure crystal at the same temperature. Below 30°K this procedure should measure the total impurity-induced absorption since the pure crystal is transparent and simply normalizes out the frequency dependence of the interferometer and detector. Above 30°K, the pure crystal is no longer completely transparent because of the temperature-dependent difference-band absorption. Some uncertainty then exists in the background level of our high-temperature data and this effect will contribute to a large experimental uncertainty in the strength of an absorption line. Moreover, because it is difficult to measure the zero level of a transformed interferogram accurately, the interferometer itself contributes an additional absolute uncertainty in the background level at all temperatures. We have been able to measure the center frequency and linewidth with increased precision but not the integrated absorption intensity under the ZPL. Our only contribution to this latter measurement is to note that all systems have been measured with the same instrument, the intensities agree with those previously reported and no new lines appear in the alkali halide crystals as the temperature is increased.

The low-temperature sample and detector cryostat used for these measurements has been described earlier.[18] It is a straightforward transmission cryostat in which the radiation passes first along a light pipe through the sample compartment then through a vacuum window to the detector chamber. The detector is a chip of gallium-doped germanium[19] with a sensitivity at 1.2°K of about 10^5 V/W.

The separation of the sample chamber from the detector chamber by the crystal quartz window made temperature-dependence measurements possible over a fairly wide range. A small amount of He^4 exchange gas coupled the samples to the bath sufficiently well so they reached a temperature of about 2°K. By removing the exchange gas and heating the sample ring with a resistance heater, sample temperatures as high as 70°K could be maintained. Even at this temperature the samples were sufficiently decoupled from the helium that the bath temperature changed by only 0.1°K. Between 30 and 70°K the detector sensitivity decreased because of this small rise in bath temperature.

The temperature was measured by determining the resistance of $\frac{1}{10}$W Allen–Bradley carbon resistor of either 1000 or 4700 Ω nominal resistance. The resistors were calibrated at boiling helium and boiling nitrogen temperature at atmospheric pressure. The resistances at these two temperatures were used to determine the constant A and B in[20]

$$T=\frac{A\log R}{(\log R-B)^2}.$$

The resistance was measured using a 25 cps ac bridge which dissipated less than 10^{-8} W in the resistor.[21]

The sample temperature was regulated by controlling the current in a nichrome wire heater. The current was controlled by a temperature regulator designed by Blake and Chase,[22] modified to operate at 25 cps, which used the bridge output as an error signal. In practice the heater current was adjusted manually to give approximately the desired temperature and then the current control was switched to the regulator. The regulator held the temperature constant to within 1%.

B. Results

Three features of the resonance have been measured as a function of temperature. They are the following: (1) the full linewidth at one-half the maximum absorption, $\Gamma(T)$; (2) the center frequency of the absorption maximum, $\Omega(T)$; and (3) the integrated absorption intensity $I(T)$ defined by Eq. (2). Most of our measurements have been made on crystals of KBr:Li^+ and NaCl:Cu^+. Isotopically pure dopants have been used so that the linewidth and resonant frequency are not masked by the presence of two closely spaced lines. The aging process described in I for KI:Ag^+ has discouraged us from devoting much time to this system and only a few measurements which are complementary to those previously reported[3] have been made. Some interesting measurements on a resonant made in MnF_2:Eu^{2+} are reported but because of problems with sample preparation the measurements are not as complete as for the alkali halide crystals.

1. KBr:Li^+

The temperature dependence of the linewidth and center frequency is shown in Fig. 1 for both the Li^6 and also the Li^7 isotope. No significant difference is observed in the temperature-dependent properties of the two isotopes. For the crystal doped with Li^6, the concentration was 2.4×10^{18} Li/cm^3. For the crystal doped with Li^7, the concentration was 2.3×10^{17} Li^+/cm^3. Although at low temperatures the linewidth

[17] I. G. Nolt, R. D. Kirby, C. D. Lytle, and A. J. Sievers, Appl. Optics **8**, 309 (1969).
[18] I. G. Nolt, R. A. Westwig, R. W. Alexander, Jr., and A. J. Sievers, Phys. Rev. **157**, 730 (1967).
[19] F. J. Low, J. Opt. Soc. Am. **51**, 1300 (1961).
[20] G. K. White, *Experimental Techniques in Low Temperature Physics* (Oxford University Press, London, 1959).
[21] W. D. Seward, Ph.D. thesis, Cornell University, 1965 (unpublished).
[22] C. Blake and C. E. Chase, Rev. Sci. Instr. **34**, 984 (1963).

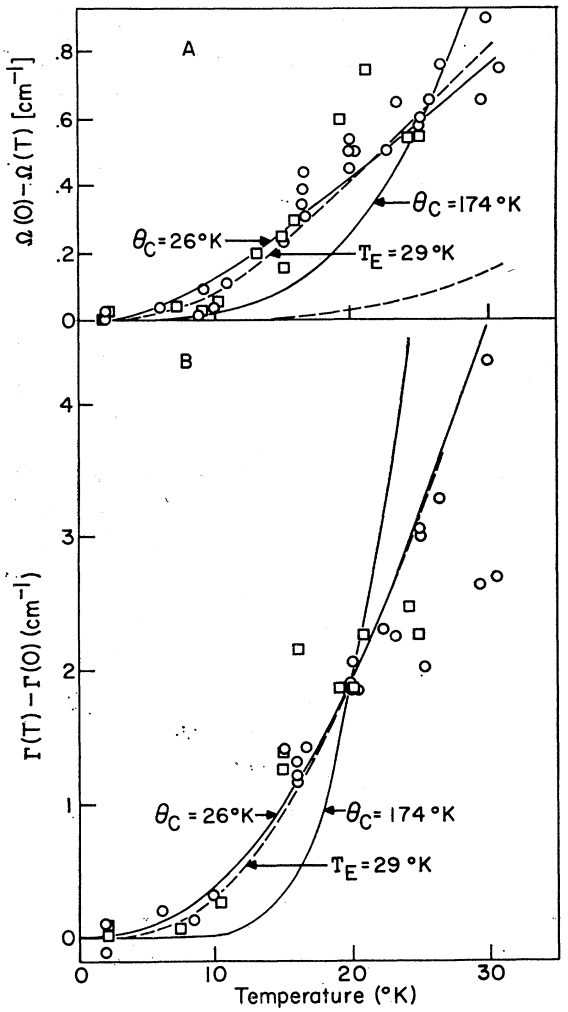

FIG. 1. (a) Temperature dependence of the center frequency of the KBr:Li^+ resonant mode. The measurements of 2.4×10^{18} $(Li^6)^+/cm^3$ are designated by the circles, and for 2.3×10^{17} $(Li^7)^+/cm^3$ by the squares. The lower dashed curve is calculated from Eq. (9). The solid curve is the sum of Eqs. (8) and (9) with $\Theta_c=26°K$ or $\Theta_c=174°K$ as indicated. The heavy dashed curve with $T_E=29°K$ is given by Eq. (23). (b) Temperature dependence of the linewidth of the KBr:Li^+ resonant mode. The circles, squares, and concentrations are the same as in 1(a). The solid curve is calculated from Eq. (7) with $\Theta_c=26°K$ and $\Theta_c=174°K$ as indicated. The heavy dashed curve with $T_E=29°K$ is given by Eq. (22).

and center frequency have been observed to depend weakly upon the concentration (see I), such an affect appears to be masked by the relatively large uncertainties in the measurements at higher temperatures. The solid and dashed curves shown in this and later figures are described in Sec. III.

Figure 2 shows the decrease in the integrated absorption strength with increasing temperature for both isotopes. By 30°K the strength is about 15% of its value at 2°K.

No difference is observed between the temperature dependence of KBr:Li^6Br and KBr:Li^7Br within the estimated experimental error of 20%. The data are in good agreement with those reported earlier.

2. *NaCl:Cu^+*

The temperature dependences of the linewidth and center frequency for NaCl:Cu^{65}Cl are shown in Fig. 3. For measurements below 30°K, the copper concentration was 1.1×10^{17} Cu^+/cm^3, while for measurements at higher temperatures a higher concentration of 6.2×10^{17} Cu^+/cm^3 was used. It was necessary to use fairly high concentrations in the sample so that the two phonon absorption would not dominate the absorption coefficient. The temperature dependences are very similar to those observed for KBr:LiBr.

As previously reported,[4] the integrated absorption strength shows a much weaker temperature dependence than observed for KBr:LiBr. Our measurements are shown in Fig. 4. At 80°K the resonant mode strength is still 60% of its value at 2°K.

3. *KI:Ag^+*

Some experimental results for KI:Ag^+ have been reported earlier.[3] The temperature dependence of the linewidth and center frequency are shown in Fig. 5. We have extended the measurements to lower temperatures and used isotopically pure silver 109 dopant. In Fig. 6 we show the temperature dependence of the

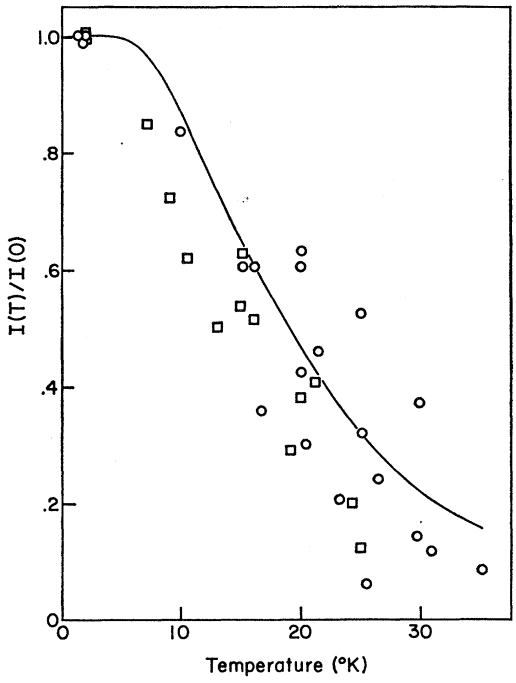

FIG. 2. $I(T)/I(0)$ versus temperature for the KBr:Li^+ resonant mode. The measurements on 2.4×10^{18} $(Li^6)^+/cm^3$ are designated by the circles, and for 2.3×10^{17} $(Li^7)^+/cm^3$ by the squares. A curve calculated from Eq. (19) with $\Omega_E=20$ cm^{-1} is also shown.

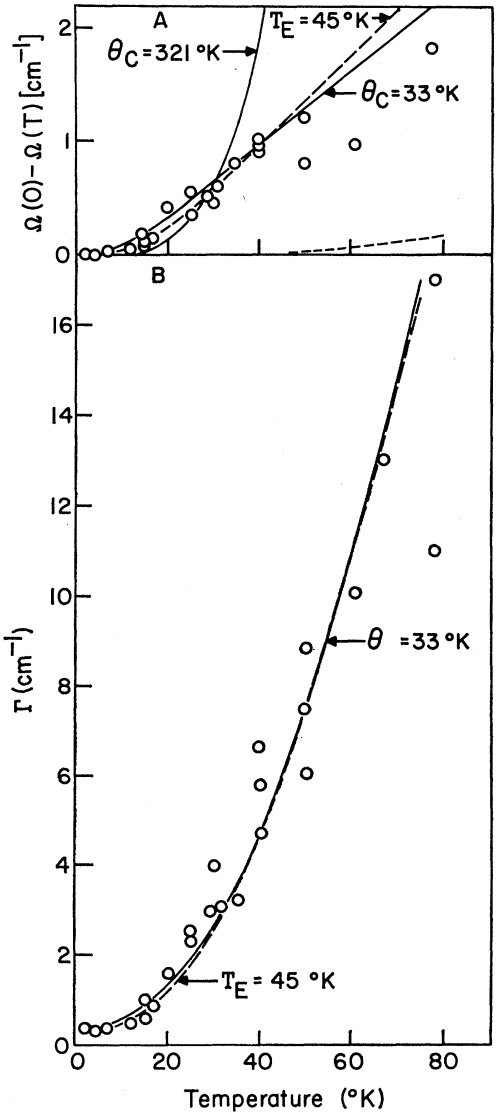

FIG. 3. (a) Temperature dependence of the center frequency of the NaCl:Cu^+ resonant mode. The dashed curve is calculated from Eq. (9). The solid curves is the sum of Eqs. (8) and (9) with Θ_c=33°K or Θ=321°K as indicated. The heavy dashed curve with T_E=45°K is given by Eq. (23). (b) Temperature dependence of the linewidth of the NaCl:Cu^+ resonance. Data below 30°K is for NaCl containing 1.1×10^{17} $(Cu^{65})^+$/cm^3, data above 30°K for NaCl containing 6.2×10^{17} (Cu^+)/cm^3. The solid curve is calculated from Eq. (7) with Θ_c=33°K. The heavy dashed curve with T_E=45°K is given by Eq. (22).

integrated absorption strength which decreases even more rapidly with increasing temperature than for KBr:LiBr. As a result of this phenomenon measurements cannot be made much above 15°K.

4. MnF_2:Eu^{2+}

The impurity-induced Eu^{2+} spectrum contains two lines superimposed on a background absorption which increases with increasing frequency. The sharpest line occurs at 16.05 cm^{-1} and the absorption spectrum is shown for 2°K in Fig. 7. The other broad line occurs at 42.1 cm^{-1}. Here we argue that the absorption line is due to a lattice resonant mode although the valance state is not known and may be either 2(+) or 3(+). The observed absorption cannot correspond to a low-lying crystal-field level because the 2(+) state has an $^8S_{7/2}$ ground state and the 3(+) ion has a singlet ground state with higher electronic levels at energies greater than 100 cm^{-1}. Because a 50-kG magnetic field shifted the absorption by less than 0.05 cm^{-1}, the absorption is not magnetic in origin. Thus we conclude that an impurity-induced resonant mode in the phonon spectrum is being observed.

For MnF_2:Eu^{2+}, two resonant modes separated in frequency are to be expected. Each threefold degenerate T_{1u} mode in a cubic crystal will split into a singly degenerate A_{2u} and a doubly degenerate E_u mode for the tetragonal MnF_2 lattice. In a previous paper[23] the absorption line at 16.05 cm^{-1} has been identified with the nondegenerate mode and the absorption line at 42.1 cm^{-1} with the other doubly degenerate resonant mode. Preliminary measurements of the temperature dependence of the low-frequency mode were reported at that time.

The spectrum at 2, 15, and 25°K is shown in Fig. 7. As the temperature of the sample is increased, the absorption strength decreases, while a shoulder begins to appear upon the high-frequency side of the line. The total area under the line plus shoulder appears to be independent of temperature. As shown in Fig. 7, the linewidth and center frequency change very slowly with temperature and an accurate measurement of these dependences has not been possible.

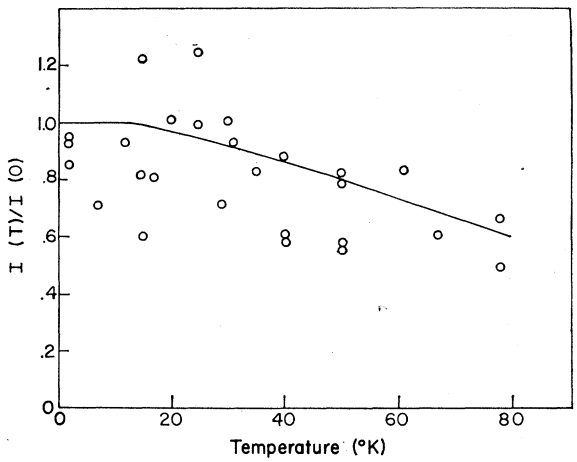

FIG. 4. $I(T)/I(0)$ versus temperature for the NaCl:Cu^+ resonant mode. The solid curve is calculated from Eq. (19) with Ω_E=31 cm^{-1}.

[23] R. W. Alexander, Jr., and A. J. Sievers, in *Optical Properties of Ions in Crystals*, edited by H. M. Crosswhite and H. W. Moos (Interscience Publishers, Inc., New York, 1967).

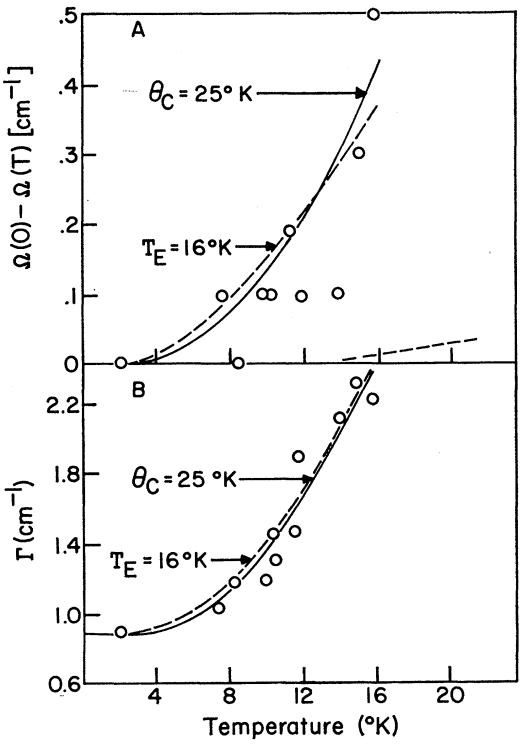

FIG. 5. (a) Temperature dependence of the center frequency of the KI:Ag^+ resonant mode. The dashed curve is calculated from Eq. (9). The solid curve is the sum of Eqs. (8) and (9) with $\Theta_c=25°K$. The heavy dashed curve with $T_E=16°K$ is given by Eq. (23). (b) Temperature dependence of the linewidth of the KI:Ag^+ resonance. Solid curve from Eq. (7) with $\Theta_c=25°K$. Data from Ref. 3. The heavy dashed curve with $T_E=16°K$ is given by Eq. (22).

III. DISCUSSION OF RESULTS

A. Temperature Dependence of Center Frequency and Linewidth

In this section we attempt to describe the various temperature-dependent effects observed in practice in terms of anharmonic effects. Anharmonic terms in the total potential energy of the system are considered in the form of powers of the normal mode coordinates Q and q, and in this context it is convenient to distinguish three different classes of terms:

(a) Terms involving only the mode Q, such as Q^3 and Q^4 (Q^3 does not occur for an odd-parity mode such as we are considering). These terms affect the energy levels of the resonant mode, but not the other lattice modes.

(b) Terms involving only the lattice modes q, such as $q'q''q'''$. Peierls[24] has shown that these can be regarded as giving rise to a temperature-dependent lattice parameter, i.e., thermal expansion.

(c) Terms involving both the resonant mode and the lattice modes, such as $Qq'q''$. These terms couple the resonant mode to the lattice modes and are referred to as coupling terms. It is through these terms that most of the effects we are considering will be discussed. Since the temperature-dependent linewidth and shift are more readily understood than the line intensity, we discuss these first.

The contribution of anharmonic terms in the potential energy to the broadening and shift of the absorption lines due to localized and resonant modes has been discussed widely in the literature, especially with reference to high-frequency localized modes.[25–30] In all these treatments the anharmonic terms have been handled by perturbation theory. To apply the results to the present data we follow the discussion by Klein.[28] The various processes contributing to the width and shift can be divided into two types: decomposition processes and scattering processes. Both can be regarded as broadening the line by limiting the lifetime of the excited resonant-mode state, and although this approach to the problem does not give detailed line shapes, etc., it does provide a simple framework for discussing features such as temperature dependence with which we are concerned.

In a decomposition process the resonant-mode excited-state decays into one or more phonons. One-phonon decays can result from anharmonic terms such as Q^3q, and schematically we can represent these by a transition

$$|1\rangle|n_q\rangle \rightarrow |0\rangle|n_q+1\rangle.$$

Conservation of energy requires, of course, $\Omega=\omega_q$. Since Ω is a low frequency where the density of phonon states is small, we expect one-phonon decays to be unimportant for resonant modes.

Two phonon decays can be of a sum or difference type, and originate from coupling terms such as $Qq'q''$. For these we can write a relaxation rate[28]

$$\frac{1}{\tau_2} = \sum_{\Omega=\omega_q+\omega_{q'}} A(q,q')(1+\bar{n}_q+\bar{n}_{q'}) + \sum_{\Omega=\omega_q-\omega_{q'}} B(q,q')(\bar{n}_q-\bar{n}_{q'}), \quad (5)$$

where A and B are the appropriate coupling coefficients and $\bar{n}$ denotes the equilibrium value of the phonon-occupation number at temperature T. In the limit of high temperature, $1/\tau_2$ is proportional to T, while for small T, $1/\tau_2$ approaches a constant.

[24] R. E. Peierls, *Quantum Theory of Solids* (Oxford University Press, London, 1956).

[25] K. H. Timmesfeld, phys. status solidi **30**, 73 (1968).

[26] A. A. Maradudin, in *Solid State Physics*, edited by F. Seitz and D. Turnbull (Academic Press Inc., New York, 1966), Vol. 19.

[27] R. J. Elliott, W. Hayes, G. D. Jones, H. F. MacDonald, and C. T. Sennett, Proc. Roy. Soc. (London) **A289**, 1 (1965).

[28] M. V. Klein, in *Physics of Color Centers*, edited by W. Beall Fowler (Academic Press Inc., New York, 1968), Chap. 7.

[29] M. A. Ivanov, M. A. Krivoglaz, D. N. Mirlin, and I. I. Reshina, Fiz. Tverd. Tela **8**, 192 (1966) [English transl.: Soviet Phys.—Solid State **8**, 150 (1966)].

[30] H. Bilz, D. Strauch, and B. Fritz, J. Phys. Rad. Suppl. **27**, C2–3 (1966).

Similarly, three-phonon decays have the limiting temperature dependence

$$1/\tau_3 \sim \text{const} \quad (\text{low } T)$$
$$1/\tau_3 \sim T^2 \quad (\text{high } T).$$

Again we expect two- and three-phonon decays to be unimportant, except possibly the difference processes such as the second term in Eq. (5), where the phonons are not restricted to low frequencies.

Scattering processes are perhaps more subtle than decomposition processes. They broaden the absorption line by limiting the lifetime of the overall excited state of the form $|1\rangle|\cdots n_q\cdots\rangle$. Schematically, the decay involved is of the type

$$|1\rangle|\cdots n_q, n_{q'}, \ldots\rangle \rightarrow |1\rangle|\cdots n_q \pm 1, n_{q'} \mp 1, \ldots\rangle,$$

and can be brought about by anharmonic terms like Q^2q (taken to second order in perturbation theory) or $Q^2q'q''$ (taken to first order). In either case these give a relaxation rate[28]

$$\frac{1}{\tau_{sc}} = \sum_{\omega_q=\omega_{q'}} C(qq')\bar{n}_q(\bar{n}_{q'}+1). \tag{6}$$

In the Debye approximation for the phonons, this expression for the line broadening becomes[7,9]

$$\Delta\Gamma_{sc}=\Gamma(T)-\Gamma(0)=\beta\left(\frac{T}{\Theta_c}\right)^7\int_0^{\Theta_c/T}\frac{x^6e^x}{(e^x-1)}dx, \tag{7}$$

where $k\Theta_c/\hbar$ is the Debye cutoff frequency. This formula demonstrates the limiting behavior of the scattering relaxation rate

$$\Delta\Gamma_{sc}\sim T^7 \quad (\text{low } T)$$
$$\Delta\Gamma_{sc}\sim T^2 \quad (\text{high } T).$$

The scattering terms also give rise to a frequency shift[27]

$$\Delta\Omega_{sc}=\Omega(0)-\Omega(T)=\delta\left(\frac{T}{\Theta_c}\right)^4\int_0^{\Theta_c/T}\frac{x^3dx}{(e^x-1)}. \tag{8}$$

There will, of course, also be a frequency shift from the anharmonic terms which give rise to thermal expansion. This contribution can be estimated through the hydrostatic strain coupling coefficient $A(A_{1g})^2$, by

$$\Delta\Omega_{ex}=A(A_{1g})[\Delta a/a(0)], \tag{9}$$

where $a(0)$ is the lattice parameter and $\Delta a=a(T)-a(0)$.

To account for the effects of thermal expansion of the lattice on the temperature dependence of the center frequency, we have used the data of White[31] for the lattice parameter $a(T)$. $\Delta\Omega_{ex}$ has been calculated form Eq. (9) using the value of $A(A_{1g})$ obtained from II. The temperature dependence is largest for KBr, which has the largest hydrostatic coupling coefficient, and is shown as a dashed line in Fig. 1(a). Somewhat smaller shifts due to thermal expansion are expected for NaCl as illustrated by the dashed line in Fig. 3(a) and for KI, by the dashed line in Fig. 5(a).

[31] G. K. White, Proc. Roy. Soc. (London) A296, 204 (1965).

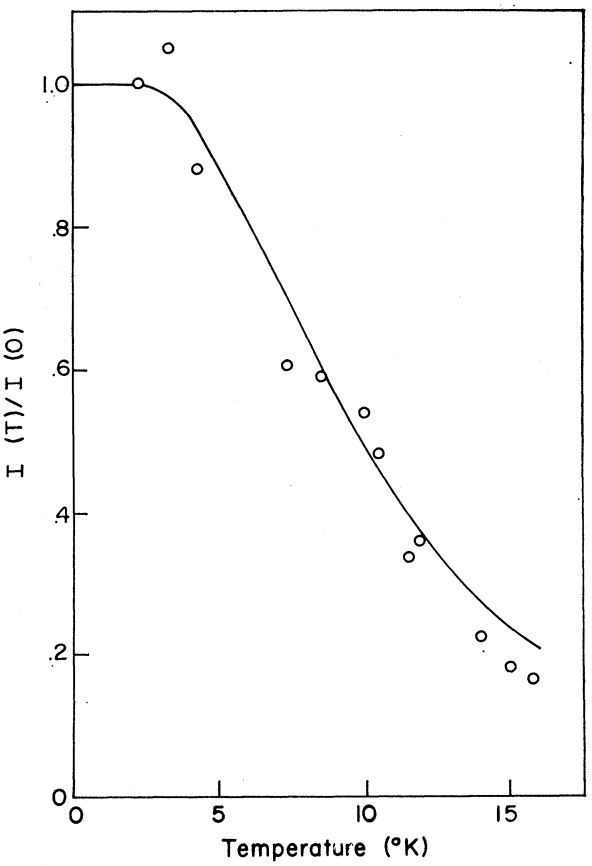

FIG. 6. $I(T)/I(0)$ versus temperature for KI:Ag^+. Solid curve is calculated from Eq. (19) with $\Omega_E=11$ cm^{-1}.

In fitting the remainder of the temperature dependence of the center position with Eq. (8) we find it

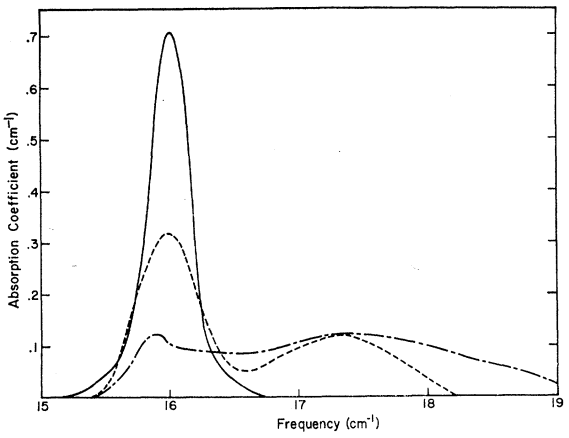

FIG. 7. Temperature dependence of the absorption coefficient in the vicinity of a resonant mode in MnF_2:Eu^{2+}. The absorption is shown for three sample temperatures. The solid curve is for 2°K, the dashed curve for 15°K, and the dash-dot curve for 25°K.

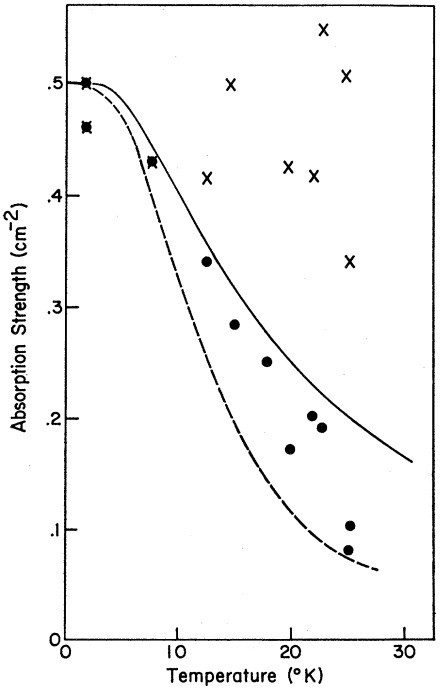

FIG. 8. Integrated absorption strength of the resonant mode in MnF_2:Eu^{2+}. The solid circles illustrate the temperature dependence of $I(T)$. The X's measure the strength of the line plus the high-frequency shoulder shown in Fig. 7. Solid curve represents the intensity for the $0 \rightarrow 1$ transition for a simple oscillator as given by Eq. (10). The dashed curve is the intensity for the $0 \rightarrow 1$ transition of a one-dimensional square well.

necessary to set $\Theta_c \approx 26°K$ for KBr:Li^+. Two calculated curves are shown in Fig. 1(a), one for $\Theta = 26°K$ and one for $\Theta_c = 174°K$, which is the Debye temperature of KBr. The smaller value of Θ_c gives a much better fit to the experimental data. In fact fits with $\Theta_c = 26 \pm 10°K$ work equally well because of the scatter in the experimental data.

It is perhaps more interesting that similar values of Θ_c must also be used for the other resonant mode systems. For NaCl:Cu^+, $\Theta_c = 33°K$ fits the experimental temperature dependence much better than setting Θ_c equal to the Debye temperature as shown in Fig. 3(a). Similarly, for KI:Ag^+ Fig. 5(a) shows that $\Theta_c = 25°K$ fits the temperature dependence of the line shift reasonably well.

To account for the temperature dependence of the linewidths we first try the scattering contribution described by Eq. (7). For KBr:Li^+ we find that a reasonable fit is obtained for $\Theta \approx 26°K$, but not for Θ_c equal to the Debye temperature. These curves are shown in Fig. 1(b). Good agreement with the experimental results is also obtained for NaCl:Cu^+ [Fig. 3(b)] and for KI:Ag^+ [Fig. 5(b)] using the same Θ_c's as found for the frequency shift.

So far we have neglected all decay processes. If decay processes are important, the significant contributions to the sums in Eq. (5) come from regions of large density of states. Weber and Nette[4] have fit the linewidth for NaCl:Cu^+ using such a two-phonon decay. Their fit requires that there be peaks in the density of states separated in frequency by the resonant-mode frequency. Because all three resonant-mode systems have essentially the same temperature dependence, it seems fortuitous that there should be density of states peaks separated by the resonant mode frequancy in all three cases. Unfortunately the difference between the scattering processes and decay processes are largest at high temperatures where the experimental uncertainty is also largest so we cannot distinguish between these two processes unambiguously.

B. Temperature Dependence of Intensity

One simple explanation of the temperature dependence of the ZLP line lies in the anharmonicity of the resonant mode itself, i.e., terms such as Q^4 in the potential. These have been shown to be important for the interpretation of electric-field experiments.[32] Terms such as these will break down the regular spacing of the harmonic oscillator levels, so that the $0 \rightarrow 1$ transition does not coincide with the $1 \rightarrow 2$ and higher transitions. If the shift in levels is larger than the linewidth of the individual transitions, then only the $0 \rightarrow 1$ transition contributes effectively to the ZLP line and its intensity will decrease as the ground state is thermally depopulated. Assuming that the anharmonicity is not too large so that we can still use the harmonic-oscillator partition function, one finds for a one-dimensional oscillator that

$$I(T)/I(0) = (1 - e^{-\hbar\Omega/kT})^2. \tag{10}$$

For a three-dimensional oscillator, on the other hand, the first-excited state is threefold degenerate but only one state is important for each polarization. Thus

$$I(T)/I(0) = (1 - e^{-\hbar\Omega/kT})^4. \tag{11}$$

$I(T)/I(0)$ as given by Eq. (10) is plotted for the resonant mode in MnF_2:Eu^{2+} in Fig. 8. To estimate the change in intensity when the anharmonicity is very large, we have also used a square-well potential for the resonant mode and plotted the intensity as the dotted line in Fig. 8. The experimental data for MnF_2:Eu^{2+} lies between these two extremes. Also from Fig. 7, the $1 \rightarrow 2$ transition may be identified as the line appearing about 1.5 cm^{-1} higher in energy than the $0 \rightarrow 1$ line. The total integrated intensity of the main line plus the side band remains essentially temperature-independent as illustrated by the X's in Fig. 8. Thus for MnF_2:Eu^{2+} the anharmonicity of the resonant mode itself gives a simple, satisfactory explanation of the temperature dependence of the absorption strength.

[32] B. P. Clayman and A. J. Sievers, Phys. Rev. Letters **21**, 1453 (1968).

Figure 9 shows a plot of the absorption strength versus temperature for KBr:Li^+, NaCl:Cu^+, and KI:Ag^+. The solid line is for a simple three-dimensional harmonic oscillator $0 \rightarrow 1$ transition as given by Eq. (11). We have normalized the temperature scale by setting $\hbar\Omega = kT_0$. For these systems it appears that the explanation in terms of the resonant mode anharmonicity does not work except perhaps for KBr:Li^+. Since other measurements of the anharmonicity of these three systems (such as the splitting of the line under a uniaxial stress[2]) suggest that all three resonances are rather similar, it is somewhat unsatisfactory to accept an explanation for KBr:Li^+ which fails disastrously for the other two. Also there is no evidence for a resolved $1 \rightarrow 2$ transition in any of these systems. Thus we suggest that anharmonicity of the resonant mode itself is not the answer for these three alkali halide modes, and instead we look for another mechanism which will produce a temperature dependence of the ZLP line.

At this point a model recently proposed by Svare[33] deserves some comment. His idea is that the Li^+ is displaced from the normal lattice site and moves in a curved potential box around this lattice site. Although he can roughly account for the observed lines at 16, 43, and 83 cm^{-1}, a weak point in his model is that it predicts a line at $(43-16)=27$ cm^{-1} to appear as the 16-cm^{-1} line disappears with rising temperature. No such line has been observed so we continue our search for the appropriate model.

Anharmonic coupling of the resonant mode to the lattice modes would appear to provide the next explanation of the ZLP intensity. However, here we come up against some problems. We have seen that the widths and shifts of the resonant mode lines can be interpreted well in terms of coupling terms, using perturbation theory to calculate the relevant expressions.

On the other hand, the changes in intensity are sometimes so large ($\Delta I/I \sim 1$) that we cannot seriously expect perturbation theory to be very useful except where the changes are small; i.e., at very low temperatures. There appear to be two methods of escape from this predicament, neither of them very satisfactory. The first is to extrapolate the results of perturbation theory blindly beyond their region of validity. This procedure has been hinted at in a number of treatments of this problem,[5,34] the idea being to write

$$I(T) = 1 - x(T) + \cdots \approx e^{-x(T)}. \tag{12}$$

This clearly has little to recommend it and we do not pursue it any further at this stage.

The second approach makes use of the well developed theory for the intensity of electronic transitions at impurities in crystals, when coupling to the lattice

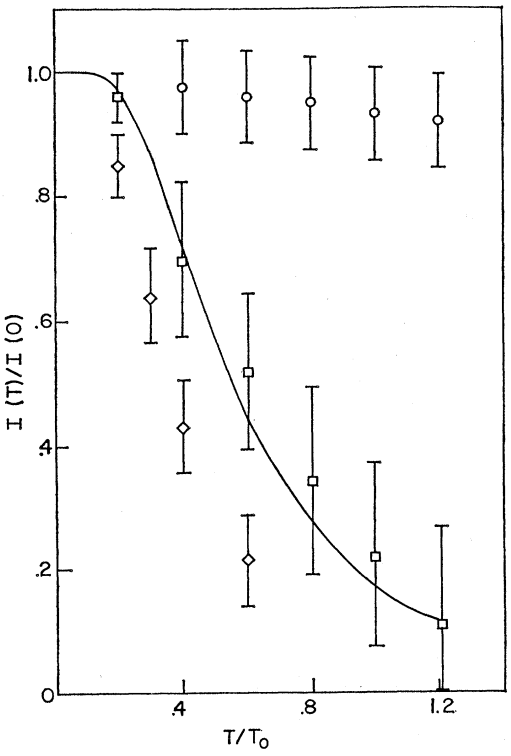

FIG. 9. $I(T)/I(0)$ versus normalized temperature (T/T_0) for three resonant mode systems, where $kT_0 = \hbar\Omega$. ○—NaCl:Cu^+, □—KBr:Li^+, and ◇—KI:Ag^+. The curve is for the three-dimensional simple-oscillator model described by Eq. (11).

modes is considered. It is not clear whether this theory can justifiably be applied to the case of a resonant mode, but nevertheless we now try to describe the experimental data in these terms.

1. Linear Coupling to a Debye Spectrum of Modes

One of the attractions of the linear coupling model is that it is possible to estimate the parameters S_q, the dimensionless linear coupling parameter, from the results of uniaxial stress measurements, since these measure the coupling of the resonant mode to lattice strains. This is outlined in *Appendix B* (see also Refs. 7 and 10). Using the Debye model for the phonons it is shown in *Appendix B* that

$$S_q = \frac{A^2(\Gamma_\alpha)}{2M_q v^2 N \hbar\omega_q}, \tag{13}$$

where $A(\Gamma_\alpha)$, is the static-strain coupling parameter for a strain of symmetry Γ_α, M_q is the effective mass of mode q, v is the Debye sound velocity, and N is the number of unit cells in the crystal. The assumption implicit in Eq. (13) is that the linear coupling to dynamic strains (phonons) is the same as to the static strain of the same symmetry. Since we are using the Debye model the appropriate effective mass for m_q

[33] I. Svare, Solid State Commun. 7, 1051 (1969).
[34] G. Benedek, in *Localized Excitations in Solids*, edited by R. F. Wallis (Plenum Press, Inc., New York, 1968).

TABLE I. $\bar{A}$ from temperature dependence of $I(T)$ and uniaxial stress measurements.

Defect system	$\bar{A}$ ($\frac{I(T)}{I(0)}$ from ln—— versus T^2 erg/unit strain)	$\bar{A}$ (from uniaxial stress using bulk elastic compliances erg/unit strain)	Θ_c
KCl R center[a]	4.6×10^{-12}	2.0×10^{-12}	157°K
KCl:H[b]	6.9×10^{-14}	2.9×10^{-14}	290°K
KBr:Li^{6}Br[c]	5.7×10^{-13}	3.5×10^{-14}	...[d]
NaCl:CuCl[c]	2.8×10^{-13}	3.5×10^{-14}	...[d]
KI:AgI[c]	7.7×10^{-13}	3.2×10^{-14}	...[d]

[a] Stress coefficients from Ref. 12.
[b] Stress coefficients from Ref. 14.
[c] Stress coefficients from Ref. 2.
[d] Θ_c cannot be determined because $I(0)/I_{\text{total}}$ is not known for resonant modes.

is the acoustic mass $m=\frac{1}{2}(m_1+m_2)$ of a diatomic lattice. Knox[35] has shown that the fraction of normal modes of point symmetry with respect to the impurity-point group is

$$f(\Gamma_\alpha)=n_\alpha^2/g+0(N^{-1/3}), \tag{14}$$

where n_α is the dimension of the irreducible representation Γ_α and g is the order of the point group. We are concerned with a point group 0_h so that the relevant $A(\Gamma_\alpha)$ are the coupling coefficient for A_{1g}, E_g, and T_{2g} strains as measured in stress experiments. Weighting each S_q according to Eq. (13), the final result is

$$I(T)=\exp\left\{-S_0\bar{A}^2\left[1+4\left(\frac{T}{\Theta_c}\right)^2\int_0^{\Theta_c/T}\frac{x\,dx}{e^x-1}\right]\right\}, \tag{15}$$

where

$$S_0=9\omega_c^2/4mv^2\hbar\omega_D^3, \quad \Theta_c=\hbar\omega_c/k \tag{16}$$

and[36]

$$\bar{A}^2=A^2(A_{1g})/48+A^2(E_g)/12+(3/16)A^2(T_{2g}). \tag{17}$$

This is obtained using a slight generalization of a Debye spectrum in which there are $3N$ normal modes with maximum frequency ω_D, but we assume that only those modes with frequency less than ω_c are coupled to the resonant mode. This is to allow for the possibility that only low-frequency modes are coupled, as was the case for the width and shift.

Note that for $T\ll\Theta_c$ we have

$$I(T)=\exp\{-S_0\bar{A}^2[1+6.6(T^2/\Theta_c^2)]\}, \tag{18}$$

i.e., a plot of $\ln I(T)$ versus T^2 should yield a straight line, a result found to hold experimentally.[3] From the slope of such a plot it is possible to calculate $\bar{A}$, since the unknown ω_c cancels in the slope. This value of $\bar{A}$ can then be compared with the value calculated from the results of uniaxial stress experiments. The results are shown in Table I, where it can be seen that the measured strain-coupling coefficients are ten times too small to explain the temperature-dependence data. Since the "Debye–Waller factor" depends on the square of the coupling coefficients, this means that the calculated temperature dependence would be 100 times too slow. Taking $\omega_c\ll\omega_D$ so that we cannot use the approximation Eq. (18), makes the disagreement worse. Thus it appears that linear coupling to a Debye spectrum of lattice modes cannot explain the temperature dependence. On the other hand, there is reasonable agreement between stress and temperature dependence data for the U center in KCl and also the R_2 band in KCl as can be seen in Table I, so perhaps the idea of correlating the two measurements does have some justification. This could, of course, simply mean that the model we have been using is inapplicable in this case, but for the time being let us assume this is only the case as far as a Debye spectrum is concerned, and pursue the linear coupling model further.

2. Linear Coupling to Other Resonant Modes

So far we have assumed that the only lattice modes coupled to the resonant mode could be represented by a Debye spectrum. This assumption was able to explain the width and shift data, where it was found that only low-frequency lattice modes were effectively coupled to the resonant mode. However, such a picture is not capable of explaining the intensity measurements, and we therefore look for a modification of the coupled mode spectrum which may be able to improve the situation.

It is known from thermal conductivity measurements that an impurity, as well as inducing an infrared active resonant mode, can induce inactive modes of similar frequency. In fact such modes have been observed in KI:Ag$^+$,[37] KBr:Li$^+$,[38] and NaCl:Cu$^+$.[39] Table II shows the frequencies determined from thermal-conductivity resonances for the inactive modes, the uncertainty in the determination being about 20%. We now assume

TABLE II. Ω_E from thermal conductivity and the value of S_E required to fit temperature dependence. [The values of Ω_E in parenthesis are those used in the fits to Eq. (18).]

Defect system	Thermal conductivity Ω_E (cm^{-1})	S_E
KBr:Li^{6}Br	31[a]	1.7 ($\Omega_E=20$ cm^{-1}, $T_E=29$°K)
KBr:Li^{7}Br	31[a]	
KI:AgI	12[b]	1.94 ($\Omega_E=11$ cm^{-1}, $T_E=16$°K)
NaCl:CuCl	46[c]	0.33 ($\Omega_E=31$ cm^{-1}, $T_E=45$°K)

[a] Reference 36. [b] Reference 37. [c] Reference 38.

[35] R. S. Knox, Solid State Commun. 4, 453 (1966).
[36] Note that $\bar{A}^2$ should be used in place of A^2 in I and that $A(A_{1g})$, $A(E_g)$, and $A(T_{2g})$ are denoted by A, B, and C, respectively, in II.
[37] F. C. Bauman and R. O. Pohl, Phys. Rev. 140, A1030 (1965).
[38] F. C. Bauman, J. P. Harrison, R. O. Pohl, and D. W. Seward, Phys. Rev. 159, 691 (1967).
[39] R. F. Caldwell and M. V. Klein, Phys. Rev. 158, 861 (1967).

that one of these modes (of even parity) is included as one of the modes q in Eq. (6). Furthermore, since the Debye spectrum of modes has been shown to be ineffective in producing temperature dependence of the intensity, we assume that we can neglect this contribution and restrict our discussion to the contributions from the even mode.

Assuming therefore just one even mode, the intensity of the ZLP line is given by

$$I(T)=e^{-\gamma_E}Z_0(C_E), \tag{19}$$

where

$$\gamma_E=S_E(2\bar{n}_E+1) \tag{20}$$

and

$$C_E=S_E\,\mathrm{csch}(\hbar\Omega_E/2kT). \tag{21}$$

In this case we must include the Bessel function $Z_0(C_E)$ since S_E is now of order unity rather than N^{-1} as for extended lattice modes. This point is discussed in the literature.[7,40]

Regarding S_E as a variable parameter we can try to fit the observed temperature dependence to Eq. (18). The results are shown in Figs. 2, 4, and 6 as solid lines. The required values of S_E are given in Table II. Some flexibility in the value of Ω_E has been allowed to improve the fit. We can push this model a little further by again trying to calculate S_E from the strain-coupling coefficients, using a somewhat different approach from that used in the discussion of the Debye model. In this case we assume that the even mode involves motion only of the defect nearest neighbors, so that we are dealing with one of the familiar normal modes of the octahedron with symmetry A_{1g}, E_g, or T_{2g}. Making an identification between the strain at the defect site and the displacement of the nearest neighbors, we can calculate (see Appendix B) the way in which the energy of the resonant-mode transition depends on the even-mode normal coordinate. This in turn gives a value for S_E corresponding to an even mode of particular symmetry. The details of a calculation such as this have also been discussed by Ham in connection with the Jahn–Teller effect,[41] where similar considerations are involved.

The results of calculating S_E in this way are shown in Table III. Two sets of numbers appear. The first set assumes that the local elastic constants are the same as those of the bulk crystal, so that the strain coupling coefficients are those given in II. The second set uses the local elastic constants calculated by Benedek and Nardelli,[42] which produce modified values of the coupling coefficients.[2,43] For each of the three systems considered there is some measure of agreement with the value of S_E from the temperature dependence data (Table II), provided one selects the most favorable choice from the three possible symmetries for the even mode. Some of the numbers are embarrassingly high, but bearing in mind the rather crude nature of the calculation the agreement is not too bad.

TABLE III. Values of S_E calculated using measured strain coupling coefficients and the cluster model of Appendix B.

Defect system	Bulk lattice compliances $S(A_{1g})$	$S(E_g)$	$S(T_{2g})$	Local compliances $S(A_{1g})$	$S(E_g)$	$S(T_{2g})$
KBr:LiBr	2.6	3.9	1.0	0.9	2.9	0.7
KI:AgI	1.9	26.1	3×10^{-3}	0.6	5.9	0.8
NaCl:CuCl	1×10^{-2}	2.4	~0	5×10^{-2}	0.23	$6\times10^{-}$

The even mode can presumably contribute to the scattering mechanism for line broadening and frequency shift since it is really several normal modes rolled into one and excitations could be scattered from one normal mode to the others. In this limit the temperature dependence of the linewidth and center frequency reduce to

$$\Delta\Gamma_{sc}=\beta'\sinh^{-2}(T_E/2T) \tag{22}$$

and

$$\Delta\Omega_{sc}=\delta'[\coth(T_E/2T)-1], \tag{23}$$

respectively. We have set $\hbar\Omega_E=kT_E$ and used the Ω_E from Table II which is required to fit the temperature dependence of the line strength to compare Eqs. (22) and (23) with experiment. The comparison is shown by the dashed line in Figs. 1, 3, and 5. By choosing β' and δ' to fit the experimental results at one temperature, good agreement is obtained over the entire temperature range measured. Thus there is some internal consistency in the idea that the active resonant mode is coupled most strongly to another resonant mode of even symmetry, and this model is at least consistent with thermal-conductivity measurements.

IV. CONCLUSIONS

We have found that the linear-coupling model using the Debye-Waller factor Eq. (3) [or Eq. (18)] is capable of explaining the temperature dependence of the ZLP line provided the active mode is coupled to another resonant mode, but not if the coupling is to a Debye spectrum of lattice modes. However, our new model of linear coupling to an even mode introduces some problems of its own. This model would predict sidebands at $\Omega\pm\Omega_E$ with strength $\sim S_E$ compared with the ZLP line. Since the S_E are ~1, it is rather awkward that no sidebands are in fact observed. One explanation, indicated by thermal-conductivity measurements, is that the even modes are broad resonances, and thus would be difficult to see in the infrared experiments. The fact that no lines are observed which increase in intensity with rising temperature to compensate for the decrease in intensity of the ZLP line is also in conflict with the general sum rule $\int\alpha(\omega)d\omega=\text{const}$, but again the effects may be too broadly distributed over

[40] D. B. Fitchen, in *Physics of Color Centers*, edited by W. Beall Fowler (Academic Press Inc., New York, 1968).
[41] F. S. Ham, Phys. Rev. **166**, 307 (1968).
[42] G. Benedek and G. F. Nardelli, Phys. Rev. **167**, 837 (1968).
[43] G. Busse, W. Prettl, and L. Genzel, Phys. Letters **27A**, 438 (1968).

the spectrum to be easily seen. Nonlinear dipole moments are a possible explanation of some of these anomalies, but so little is known of their relevant magnitudes that no firm conclusions can be drawn here.

Even accepting these drawbacks, we still have to try and justify the use of the linear coupling model, i.e., the use of the Debye-Waller factor and the analogy with the treatment of electronic transitions. For a vibrational system there can be no terms purely linear in the q's in the potential, since these are already incorporated in the harmonic Hamiltonian. Any "linear" coupling must therefore originate in anharmonic terms, but since these will contain both Q and q, they will, in general, not only couple the resonant mode to the other modes, but also couple different levels of the resonant mode itself. One of the basic assumptions of the electronic theory is that the coupling does not mix the electronic states, but only couples them to the lattice modes, so that here there is a clear difference between the two situations. The lowest order anharmonic coupling term linear in q is of the form Q^2q, and it is this term which has received most attention as a candidate for producing a Debye-Waller factor. In fact, it can be shown[15,16] that this term does result in an expression like Eq. (3), but only if $\Omega \gg \omega_q$, i.e., for high-frequency localized modes. If this condition is not met then the mixing terms become important, and it does not seem possible to carry through the proof which results in the Debye-Waller factor.

Thus the analogy does not seem to hold for resonant modes, where $\Omega \sim \omega_q$. All that can be done in this case is to resort to perturbation theory, which gives as a leading term

$$\int_{\text{ZLP}} \alpha(\omega)d\omega = 1 - \sum_q 4S_q'\Omega\left\{\frac{(\bar{n}_Q+\bar{n}_q+1)(\Omega+\omega_q)}{(2\Omega+\omega_q)^2} + \frac{(\bar{n}_q-n_Q)(\Omega-\omega_q)}{(2\Omega-\omega_q)^2}\right\}, \quad (24)$$

where S_q' is again a dimensionless coupling parameter analogous to S_q in Eq. (4). Note that the above expression is somewhat different from the one given in Ref. 15, where the transition probability rather than the absorption coefficient was calculated. Since the latter is proportional to the transition probability multiplied by the frequency, terms in the lineshift must be taken into account. It can be seen that Eq. (24) reduces to the leading term in the expansion of the Debye-Waller factor in the limit $\Omega \gg \omega_q$. There may be other conditions under which the leading term has a temperature dependence like $(2\bar{n}_q+1)$, for example, if $\Omega=\omega_q$. However, we prefer not to speculate further on similarities between the perturbation theory and the Debye-Waller factor, but rather remark that as an empirical expression the latter seems to work, provided coupling to an even resonant mode is assumed. This approach not only explains the temperature dependence, but also gives reasonable correlation with coupling coefficients measured in static-stress experiments. It remains to be shown whether the agreement is fortuitous, or whether it is firmly based on a (as yet undeveloped) complete theory of anharmonic properties of low-frequency resonant modes.

ACKNOWLEDGMENTS

We should like to thank Professor J. B. Page for interesting discussions. One of us (A.E.H.) would like to express his sincere gratitude to the Commonwealth Fund of New York for the award of a Harkness Fellowship.

APPENDIX A: SUM RULE $\int_0^\infty \alpha(\omega)d\omega = \text{CONST}$

Strauch[5] has proved this sum rule for an anharmonic system with a linear dipole moment, using the anharmonic one-phonon Green's function. We wish to present here an alternative simple proof of the theorem.

The Hamiltonian we consider is expressed in terms of harmonic normal modes Q and q, and has the form

$$H = H(Q)+H(q)+H'(Q,q),$$

where $H(Q) = -(\hbar^2/2M_Q)\nabla_Q^2 + kQ^2$ etc., and $H'(Q,q)$ is the anharmonic part of the potential.

We take the dipole moment to be $M=zQ$, where z is an effective charge.

Allowing for negative contributions from stimulated emission, the absorption coefficient may be written (ignoring multiplicative constants)

$$\alpha(\omega) = Av_i \sum_f |\langle f|M|i\rangle|^2 \omega_{fi}\delta(|\omega_{fi}|-\omega), \quad \text{(A1)}$$

where $\omega_{fi}=(E_f-E_i)/\hbar$. $|i\rangle$ and $|f\rangle$ are eigenstates of H with eigenvalues E_i and E_f, and Av_i indicates a thermal average over the states $|i\rangle$.

By expanding the commutator $[Q,[H,Q]]$ it is straightforward to show that

$$\sum_f (E_f-E_i)|\langle f|Q|i\rangle|^2 = \hbar^2/2M_Q \quad \text{for all } i. \quad \text{(A2)}$$

This may be recognized as a disguised version of the Thomas–Reich–Kuhn f sum rule in atomic spectra.

Combining (A1) and (A2) it follows that

$$\int_0^\infty \alpha(\omega)d\omega = \hbar z^2/2M_Q = \text{const}.$$

It is trivial to generalize the result to the case of an arbitrary number of active modes, the result being

$$\int_0^\infty \alpha(\omega)d\omega = \hbar \sum_i z_i^2/2M_i$$

in an obvious notation.

APPENDIX B: RELATION BETWEEN STRAIN COUPLING COEFFICIENTS AND HUANG–RHYS FACTORS

1. Debye Model

This is most simply illustrated by considering a one-dimensional chain. The displacement of atom n is given in terms of the normal modes q by

$$u_n=\frac{1}{\sqrt{N}}\sum_q qe^{ik_qna}, \tag{B1}$$

where a is the unit cell length and N is the number of unit cells. The strain at $n=0$ is therefore

$$\epsilon=\frac{u_1-u_0}{a}=\frac{1}{a\sqrt{N}}\sum_q q(e^{ik_qa}-1)$$

$$\approx\frac{i}{\sqrt{N}}\sum_q k_qq \quad \text{for long wavelengths } k_qa\ll 1. \tag{B2}$$

Thus we can identify, in the long wavelength limit, a strain

$$\epsilon_q=k_qq/\sqrt{N} \tag{B3}$$

with mode q. The phase factor i may be ignored.

We define a strain coupling coefficient for symmetry Γ_α by the equation

$$\Delta E_\alpha=A(\Gamma_\alpha)\epsilon_\alpha, \tag{B4}$$

where ΔE_α is the change in transition energy for strain ϵ_α.

From (B3) and (B4) we can therefore write the change in transition energy linear in q as

$$\Delta E_q=\frac{A(\Gamma_\alpha)}{\sqrt{N}}k_qq. \tag{B5}$$

In the linear-coupling theory,[7] the transition energy is assumed to depend on q through a term

$$\Delta E_q=C_qq, \tag{B6}$$

and with this definition the Huang–Rhys factors are given by

$$S_q=C_q^2/2m_q\hbar\omega_q^3. \tag{B7}$$

From (B5) and (B6) it follows that

$$S_q=A^2(\Gamma_\alpha)/2m_qv^2N\hbar\omega_q, \tag{B8}$$

where v is the Debye sound velocity $(=\omega_q/k_q)$.

The approximation $C_q\propto\omega_q$ is discussed in great detail using alkali halide normal modes by Maradudin.[7]

2. Cluster Model

In this model we assume that only coupling to the nearest neighbors is important in both static stress experiments and the dynamic case. Consider for example the A_{1g} "breathing mode" of the octahedron, and suppose each neighbor moves a distance X towards the impurity. The compressive strain is then given by

$$\epsilon_{xx}=\epsilon_{yy}=\epsilon_{zz}=X/a, \tag{B9}$$

where a is the nearest-neighbor distance.

In the breathing mode the normal coordinate q_1 is related to X by

$$q_1=1/\sqrt{6}(X_1+X_2+X_3+X_4+X_5+X_6), \tag{B10}$$

where X_1 is the displacement of ion 1, etc., and in this normalized form the effective mass of the mode q_1 is the nearest neighbor mass m.[41]

Clearly we have, since $X_1=X_2=X_3$, etc. $=X$:

$$q_1=\sqrt{6}X \tag{B11}$$

so that

$$\epsilon_{xx}=q_1/a\sqrt{6}. \tag{B12}$$

(B12) is analogous to (A5).

In a stress experiment we have[2]

$$\Delta E_{A_{1g}}=A(A_{1g})(\epsilon_{xx}+\epsilon_{yy}+\epsilon_{zz}) \tag{B13}$$

so that it follows from (B12), (B6), and (B8) that

$$S(A_{1g})=\frac{3A^2(A_{1g})}{4m\hbar\Omega_A^3a^2}, \tag{B14}$$

where Ω_A is the frequency of the A_{1g} mode.

The analogous expressions for E_g and T_{2g} modes are

$$S(E_g)=\frac{6A^2(E_g)}{m\hbar\Omega_E^3a^2} \tag{B15}$$

and

$$S(T_{2g})=\frac{2A^2(T_{2g})}{3m\hbar\Omega_T^3a^2}. \tag{B16}$$

The numerical factors result from considerations such as those leading up to (B11) (see, for example, Ref. 41).